



**HAL**  
open science

# Acoustic source detection inside a pipe using vibro-acoustic beamforming: assessment of the array gain from virtual experiments

Souha Kassab, Sanae Serbout, Frédéric Michel, Laurent Maxit

## ► To cite this version:

Souha Kassab, Sanae Serbout, Frédéric Michel, Laurent Maxit. Acoustic source detection inside a pipe using vibro-acoustic beamforming: assessment of the array gain from virtual experiments. ICA 2019, Sep 2019, Aachen, Germany. hal-02414585

**HAL Id: hal-02414585**

**<https://hal.science/hal-02414585>**

Submitted on 16 Dec 2019

**HAL** is a multi-disciplinary open access archive for the deposit and dissemination of scientific research documents, whether they are published or not. The documents may come from teaching and research institutions in France or abroad, or from public or private research centers.

L'archive ouverte pluridisciplinaire **HAL**, est destinée au dépôt et à la diffusion de documents scientifiques de niveau recherche, publiés ou non, émanant des établissements d'enseignement et de recherche français ou étrangers, des laboratoires publics ou privés.

## Acoustic source detection inside a pipe using vibro-acoustic beamforming: assessment of the array gain from virtual experiments

Souha Kassab<sup>1,2</sup>, Sanae Serbout<sup>1,2</sup>, Frédéric Michel<sup>2</sup>, Laurent Maxit<sup>1</sup>

<sup>1</sup>Laboratoire Vibrations-Acoustique (LVA), INSA Lyon, Villeurbanne, France

<sup>2</sup>DTN/STCP/LISM, Commissariat of Atomic Energy and Alternative energies, Cadarache, France

### ABSTRACT

In the R&D framework on sodium water heat exchangers, a monitoring technique based on vibration measurements is developed for detecting a leak of water into the sodium. However, leak-induced vibrations could be smeared in the ambient vibrations. In order to increase the signal-to-noise ratio (SNR), the conventionnel and MaxSNR beamforming treatments have been considered. In order to study their efficiency for the present application, one has developed a laboratory mock-up composed by a pipe coupled to a hydraulic circuit through two flanges. The source to detect is a sound emitter introduced into the pipe whereas the background vibration noise is controlled by changing the speed of the flow. In parallel, numerical vibro-acoustic tools were developed for predicting the vibratory response of the pipe excited by a monopole source or a turbulent boundary layer. These models allow us to realize virtual experiments mimicking the behavior of our laboratory test case. The virtual signals induced by the monopole source to be detected and by the turbulent flow are used for assessing the performances of the vibro-acoustic beamforming treatments. After a presentation of the vibro-acoustic models, we illustrate the array gain estimated using the virtual experiments for the two beamforming treatments.

Keywords: beamforming, detection, pipe, vibro-acoustic modeling

### 1. INTRODUCTION

This paper describes the study of a non-intrusive vibro-acoustic beamforming technique aimed at the detection of sodium-water reactions in the steam generator of a liquid sodium fast reactor (SFR). Vibro-acoustic beamforming previously developed within a PhD thesis by J. Moriot is reconsidered [1]. Beamforming over an array of sensors is of main interest due to its ability to increase the signal to-noise ratio (SNR) of the chemical reaction signals, generally masked by the high power plant background noise. Thus, we can provide a quantitative estimation of the SNR increase at the beamforming output relative to the SNR on the reference sensor using the “effective gain”. From the detection on a threshold criterion at the output of beamforming (instead of the reference sensor), this gain allows the improvement of the detection rate while limiting the sensibility to false alarms. Moriot’s thesis showed promising results. However, the latter were obtained by on academic numerical test models (plate or infinite shell) or from experimental data at some harmonic frequencies [2]. New investigations have been carried out in the framework of the Kassab thesis in order to assess more accurately the interest of the vibro-acoustic beamforming for detecting an acoustic source inside a pipe. Numerical models of the pipe test section illustrated in the figure 1 have been developed. In these models, the coupling between the pipe and the flanges is described as well as the coupling between the pipe and the inner fluid (water). These models allows us to simulate the vibrations on the pipe excited, either by a monopole source or by a turbulent flow. These simulations allows us generating virtually the array signals due to the source to be detected (i.e. a monopole) and due to the background noise (i.e. turbulent flow). From these virtual signals, one can test different types of beamforming treatments and different physical/array parameters. In the section 2, one recalls the principle of two types of beamforming treatments whereas the theoretical principles of the vibro-

acoustic simulations are presented in section 3. An illustration of the treatments of the virtual experiment data is proposed in section 4.

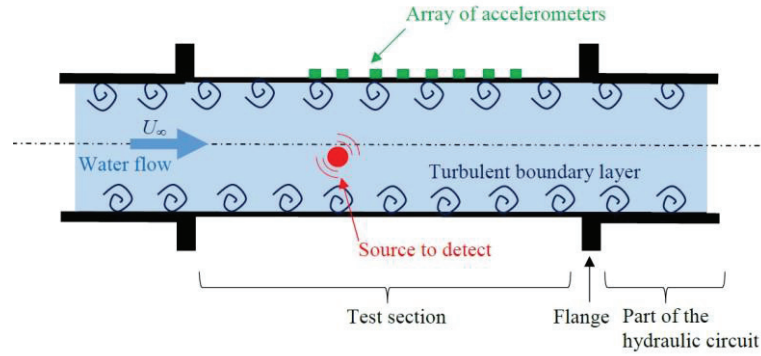


Figure 1. Schematic representation of the configuration considered for assessing the performance of the vibro-acoustic beamforming

## 2. CLASSICAL AND MAXSNR BEAMFORMING

In this section, one recalls the principle of two beamforming treatments that will be evaluated on the pipe test section through virtual experiments.

Let us denote by  $\Gamma$  the cross-spectral matrix of the signals received by the array of sensors and by  $F_u$  the steering vector (i.e. spatial filtering vector) when the treatment focus at the position  $u$  of the detection space. The beamforming output,  $y_u$  is given by:

$$y_u = F_u^* \Gamma F_u. \quad (1)$$

Assuming that the source to be detected and the background noise are independent, we can decompose the matrix  $\Gamma$  as such:

$$\Gamma = \Gamma^s + \Gamma^n, \quad (2)$$

where  $\Gamma^s$  is the cross-spectral matrix of the signals induced by the source alone and  $\Gamma^n$  is the cross-spectral matrix of the signals induced by the noise alone.

When the background noise is spatially homogeneous and incoherent (i.e.  $\Gamma_b = \sigma_b I$  with  $I$  the identity matrix and  $\sigma_b$ , the power spectrum density of the background noise), it can be shown that the array gain is maximum when the steering vector is given by:

$$F_u^{class} = \frac{H_u}{\|H_u\|}, \quad (3)$$

where  $\| \cdot \|$  represents the Euclidean norm and  $H_u$  is the vector containing the transfer functions between the (assumed) position  $u$  of the source and the antenna's accelerometers (i.e. sensors).

This beamforming technique relies on a prior knowledge of the source (through the transfer functions) as well as on the assumption that the noise would appear spatially incoherent. In the following, one refers as the classical beamforming for this treatment.

The classical beamforming is widely used in the world for various applications. However, when the background noise is partially correlated (spatially), its performances can be strongly deteriorated compared to those obtained when the noise is perfectly incoherent.

To overcome this drawback, different variants of beamforming based on prior knowledge on the noise have been developed [3]. In particular, the so-called MaxSNR beamforming seeks to maximize the signal-to-noise ratio at the beamforming output, knowing the cross-spectral matrix of the noise.

The steering vector is then defined as follows:

$$F_u^{opt} = \underset{F_u}{\operatorname{argmax}} \left[ \frac{F_u^* \Gamma_u^S F_u(\omega)}{F_u^* \Gamma^n F_u(\omega)} \right], \quad (4)$$

where  $\Gamma_u^S$  is the cross-spectral matrix of the signals induced by the source located at the position  $u$  in the detection space.

From bilinear algebra considerations, it can be shown that the solution of Eq. (4) corresponds to one eigenvector associated with the greatest eigenvalue of the matrix  $(\Gamma^n)^{-1} H_u H_u^*$ :

$$(\Gamma^n)^{-1} H_u H_u^* F_u^{opt} = \lambda_{max} F_u^{opt}. \quad (5)$$

This treatment can be relevant for the source detection in the pipe with a threshold criteria as it permits to increase the SNR at the output of beamforming compared to the one of a single sensor. Nevertheless, this technique requires solving a generalized eigenvalues problem which can induce numerical instabilities. It also requires knowledge of the cross-spectral matrix of the noise. In practice, this can be estimated from *in-situ* measurements with the sensor array when the source is (supposed) off. An average over a set of measured signals samples can be performed regularly to take into account the variation of the cross-spectral noise matrix in the system as a function of time.

### 3. VIRTUAL EXPERIMENTS

In this section, one presents briefly the principle of the numerical simulations for generating the sensor signals induced by the monopole source to be detected and by the turbulent flow constituting the background noise.

#### 3.1 Vibratory response of the shell excited by a monopole source

##### 3.1.1 Circumferential admittance approach

One considers the system shown in Figure 1-a composed of an infinite cylindrical shell filled with a heavy fluid (water) and coupled to two ring stiffeners. In this section, one supposes that the system is excited either by a monopole inside the fluid or by a radial point force applied on the shell. The excitation is supposed harmonic with a time dependency in  $e^{j\omega t}$  where  $\omega$  represents the angular frequency. The dynamic behavior of the thin cylindrical shell will be described by the Flügge model whereas the acoustic behavior of the fluid will be represented by the Helmholtz model. Only the coupling along the radial direction between the shell and the stiffener will be considered for these first developments. The ring stiffener will be represented by a ring model (i.e. rod of circular curvature). A cylindrical coordinate system  $(x, r, \theta)$  is considered. The two ring stiffeners are located at the axial positions,  $x_1$  and  $x_2$ .

The global system is partitioned in two subsystems as shown in Figure 2. The fluid filled cylindrical shell constitutes one subsystem whereas the ring stiffeners constitutes the second subsystem.

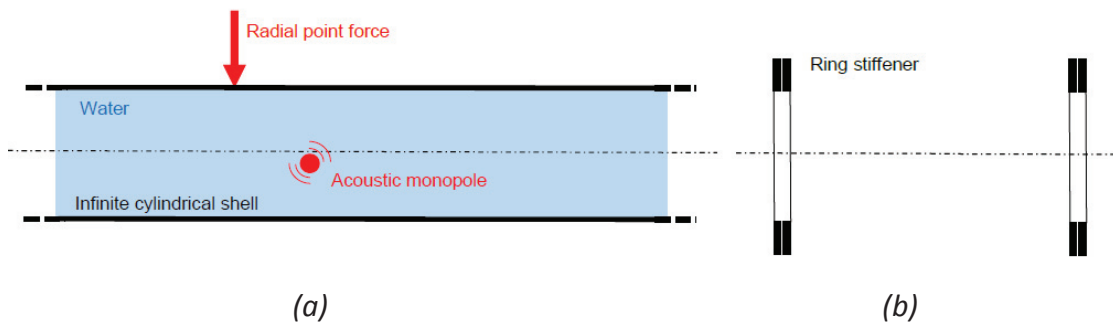


Figure 2. Partitioning of the vibro-acoustic problem: (a), fluid filled cylindrical shell; (b), ring stiffeners.

One will use the circumferential admittance approach (CAA) [4] for assembling the two subsystems. One reminds here the principle of the approach (for more details, see [4]).

• First, as the considered system is axisymmetric (excepted for the excitation), the different spatial fields (displacement, acoustic pressure, force) noted  $f$  can be represented by a Fourier series decomposition about the circumference:

$$f(\theta) = \sum_{n \in \mathbb{Z}} \tilde{f}(n) e^{jn\theta}. \quad (6)$$

• Second, for each circumferential order  $n$  (omitted of the notation in the following), one defines the circumferential admittances  $\tilde{Y}_{ij}^\alpha$  ( $\text{m}^2/\text{N}$ ) of the shell ( $\alpha=1$ ) and of the ring stiffeners ( $\alpha=2$ ) between the junction  $i$  and  $j$  by:

$$\tilde{Y}_{ij}^\alpha = \frac{\tilde{W}_{i,j}^\alpha}{\tilde{F}_i^\alpha}, i \in \{1,2\}, j \in \{1,2\}, \quad (7)$$

where:

- $\tilde{W}_{i,j}^\alpha$  ( $\text{m}$ ) is the circumferential radial displacement at the junction  $j$  (of the shell for  $\alpha = 1$  or of the stiffeners for  $\alpha = 2$ ) for a circumferential radial force applied at junction  $i$ ;
- $\tilde{F}_i^\alpha$  ( $\text{N/m}$ ) is the circumferential radial force applied at junction  $i$  on the shell by the stiffeners for  $\alpha = 1$  or the circumferential radial force applied on the stiffeners by the shell for  $\alpha = 2$ .

Moreover, for each subsystem  $\alpha$ , one defines the circumferential free displacement at the junction  $i$ ,  $\tilde{W}_i^\alpha$  as the circumferential radial displacement induced by the external excitation at the junction  $i$  when all the junctions are let free

• Finally, using the superposition principle for passive linear systems and considering the radial displacement continuity and the force equilibrium at the junctions, one finally obtains the matrix system [4]:

$$(\tilde{Y}^1 + \tilde{Y}^2) \tilde{F}^c = \tilde{W}^1 - \tilde{W}^2, \quad (8)$$

$$\text{where } \tilde{Y}^\alpha = \begin{bmatrix} \tilde{Y}_{11}^\alpha & \tilde{Y}_{12}^\alpha \\ \tilde{Y}_{21}^\alpha & \tilde{Y}_{22}^\alpha \end{bmatrix}, \tilde{F}^c = \begin{bmatrix} \tilde{F}_1^c \\ \tilde{F}_2^c \end{bmatrix}, \tilde{W}^\alpha = \begin{bmatrix} \tilde{W}_1^\alpha \\ \tilde{W}_2^\alpha \end{bmatrix}.$$

Resolving this equation system, one deduces the coupling forces exerted by the stiffeners on the shell. In a last step, one can introduce these forces in the model of the infinite fluid filled shell in order to estimate the vibratory field of the shell when it is coupled to the ring stiffeners. In the following, as no external excitation is contained in subsystem #2, one considers that  $\tilde{W}_i^2 = 0$  in Eq. (4).

### 3.1.2 Spectral approach for estimating the shell circumferential admittance and free displacement

The problem describing the vibro-acoustic behaviour of the fluid loaded shell excited by a harmonic radial force is resolved using a spectral approach. The 2D Fourier transform (i.e. space Fourier transform about  $x$ -axis + Fourier serie decomposition about the circumference) is considered:

$$f(x, \theta) \rightarrow \tilde{f}(k_x, n, \omega) = \frac{1}{2\pi} \int_{-\infty}^{+\infty} \int_0^{2\pi} f(x, \theta) e^{-jk_x x} e^{-jn\theta} d\theta dx \quad (9)$$

where  $f$  is a generic function representing either the shell displacements or the acoustic pressure.

Applying this transform to the Flügge, Helmholtz, and Euler equations describing the behaviour of the fluid filled shell, one obtains finally [4]

$$\tilde{W} = \gamma \tilde{F}_w \frac{\tilde{Z}_{uu} \tilde{Z}_{vv} - (\tilde{Z}_{uv})^2}{\tilde{\Delta}}, \quad (10)$$

where  $\tilde{Z}_{\zeta\xi}$  are the components of the spectral Flügge matrix,  $\tilde{\Delta}$  is the determinant of the spectral Flügge matrix taking into account of the spectral fluid loading impedance and  $\gamma$  is a constant depending on the shell characteristics.

In order to estimate the circumferential admittances of the fluid filled cylindrical shell, one considers the shell excited by a radial circumferential force at  $x=0$  of unit magnitude for each circumferential order,  $n$ . As the considered system is invariant in translation about the axial direction,

the admittance between junctions i and j can be deduced from

$$\tilde{Y}_{ij}^1 = \frac{\tilde{W}(x_i - x_j, n)}{\tilde{F}}, \quad (11)$$

where  $\tilde{W}$  is the radial displacement of the shell excited by a unitary radial circumferential force  $\tilde{F}$  at  $x=0$  ( $\tilde{F}=1$  N/m).

The spectral radial force for the unitary circumferential radial force applied at  $x=0$  is  $\tilde{F}_w = 1$  N/m. The spectral radial displacement  $\tilde{W}$  can then be calculated analytically using Eq. (6). The circumferential displacement  $\tilde{W}$  can be obtained from an inverse Fourier transform about  $x$ .

### 3.1.3 Model of the ring stiffener

As the two stiffeners are not physically coupled, one has  $\tilde{Y}_{12}^2 = \tilde{Y}_{21}^2 = 0$  and as they are identical,  $\tilde{Y}_{11}^2 = \tilde{Y}_{22}^2 = \tilde{Y}_r$ . Each ring is represented by a rod of circular curvature and of rectangular cross-section.  $l_r, h_r, \rho_r, c_r$  represent the width, height of the cross section, density of the material and celerity of the extensional waves. Neglecting inertia and rotary effect, one can determinate its circumferential admittance,  $\tilde{Y}_r$  (m/N) as given in reference [5].

### 3.2 Vibratory response of the shell excited by the turbulent flow

Now let us considered the fluid filled shell excited by a turbulent flow. The flow speed is supposed to be low compared to the acoustic speed and the turbulent boundary layer (TBL) excited the wall of the shell is supposed homogeneous, stationary and fully developed. The effect of the convection on the acoustic behaviour is neglected. The Cross Spectrum Density (CSD) of the Wall Pressure Field (WPF) induced by the TBL,  $\phi_{pp}$  will be estimated from the TBL parameters and a mixed Goody-Chase 1987 model [6,7]. The CSD of the radial shell displacement between the points of coordinates  $(x, \theta)$  and  $(x', \theta')$ ,  $S_{ww}^R$  can be written (see [8-12]):

$$S_{ww}^R(x, \theta, x', \theta', \omega) = 2\pi \sum_{n=-\infty}^{+\infty} \int_{-\infty}^{+\infty} \tilde{H}_w^{\omega*}(x, \theta, k_x, n) \phi_{pp}^R(k_x, n, \omega) \tilde{H}_w^{\omega}(x', \theta', k_x, n) dk_x. \quad (12)$$

where the sensitivity functions,  $\tilde{H}_w^{\omega}$  are expressed (using the reciprocity principle as described in [8, 10]),

$$\tilde{H}_w^{\omega}(x, \theta, k_x, n) = \frac{1}{2\pi} \int_{-\infty}^{+\infty} \int_0^{2\pi} H_w(\tilde{x}, \tilde{\theta}, x, \theta, \omega) e^{-jk_x \tilde{x}} e^{-jn\tilde{\theta}} d\tilde{x} d\tilde{\theta}. \quad (13)$$

In Eq. (13),  $H_w(\tilde{x}, \tilde{\theta}, x, \theta, \omega)$  corresponds to the radial displacement of the shell at point  $\tilde{M}$  of coordinates  $(\tilde{x}, \tilde{\theta})$  when the shell is excited by a unitary radial point force at point M of coordinates  $(x, \theta)$ . Considering the definition of the Fourier transform given by Eq. (9), its results that the sensitivity functions  $\tilde{H}_w^{\omega}$  given by Eq. (13) correspond to the Fourier transform of the shell radial displacement field (expressed in  $(k_x, n)$  space) when the shell is excited by a unitary radial point force at point M. For the fluid filled shell coupled to the two ring stiffeners, these quantities can be calculated using the CAA approach described in section 2. For calculating the sensitivity functions at a given point M, it is necessary to consider a unitary radial point force at this point, to calculate the coupling forces by resolving Eq. (8), and to evaluate the spectral radial displacement of the shell directly from Eq. (10).

The CSD of the radial displacement excited by the TBL can then be estimated using Eq. (12), the sensitivity functions  $\tilde{H}_w^{\omega}$  estimated with the CAA approach and the CSD of the WPF,  $\phi_{pp}^R$  given the Goody-Chase model  $\phi_{pp}$ .

#### 4. ASSESSMENT OF THE BEAMFORMING TREATMENTS USING VIRTUAL EXPERIMENT

Only an illustration of the beamforming assessment with the virtual experiment data obtained with the models developed in section 3 is presented. More results will be presented during the oral presentation and will be published in an international journal.

The test section is composed by a cylindrical shell made of stainless steel and filled with water. The length, the diameter and the thickness are respectively, 3.1 m, 219 mm and 8 mm. The vibrations are measured by a linear array of 24 *virtual* accelerometers fixed on the pipe. The spacing between the sensors is  $\Delta x = 4$  cm and the first accelerometers is positioned at 15 cm from the upstream flange of the flow.

Figure 3 shows the acceleration levels at the sensor position for two positions of the source. The patterns appearing on this figure are due to the circumferential and pseudo-axial modes of the pipe.

Figure 4a illustrates the acceleration levels at the sensor position for a turbulent flow whereas figure 4b presents the coherence between sensor #12 and the other sensors for the same turbulent flow. One can observe the signals due to the background noise may be significantly correlated at certain frequencies.

The data related to the two previous figures have been filtered by the two beamforming treatments described in section 2. One illustrates one result of these treatments by showing the array gain for a wide band analysis. This gain expresses the increase of SNR by the beamforming compared to the SNR on the reference sensor. This result shows that the interest of the classical beamforming is weak for this case, with a negative gain at some frequencies and a gain always lesser than 4 dB (due to the strong coherence of the background noise) whereas a significant gain, over 18 dB in mean, is obtained with the MaxSNR beamforming, whatever the frequency band.

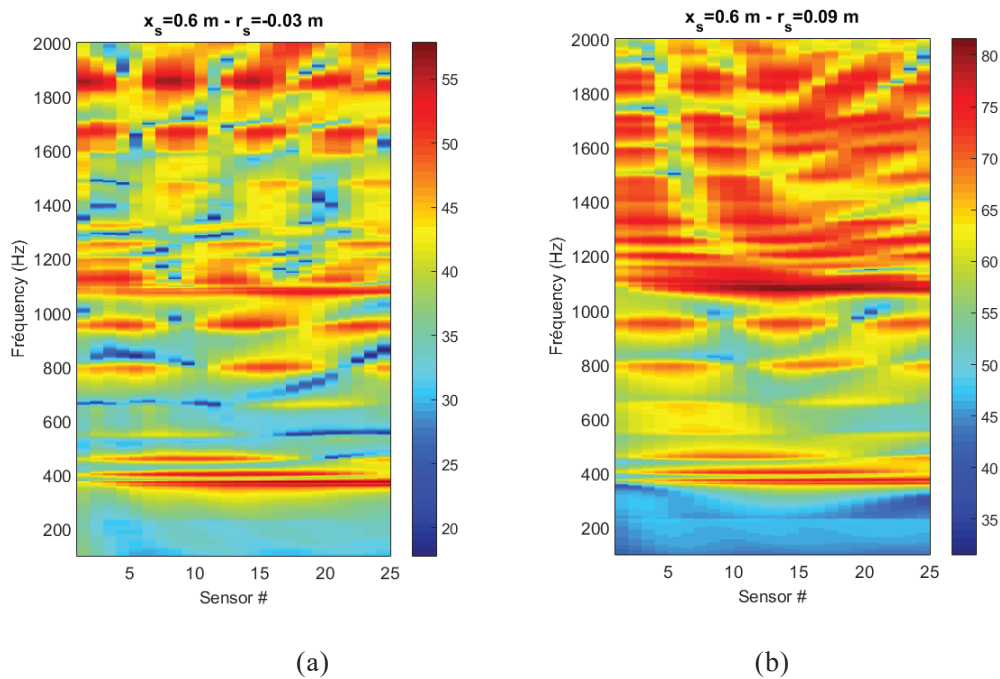


Figure 3. Acceleration levels (ref. dB,  $1 \mu\text{m}\cdot\text{s}^{-2}\cdot\text{Hz}^{-0.5}$ ) measured by the sensor array for two radial positions of the acoustic source: (a),  $r_s = -0.03$  m; (b),  $r_s = 0.09$  m.  $x_s = 0.6$  m,  $\theta_s = 0^\circ$ . Results of CAA calculation.

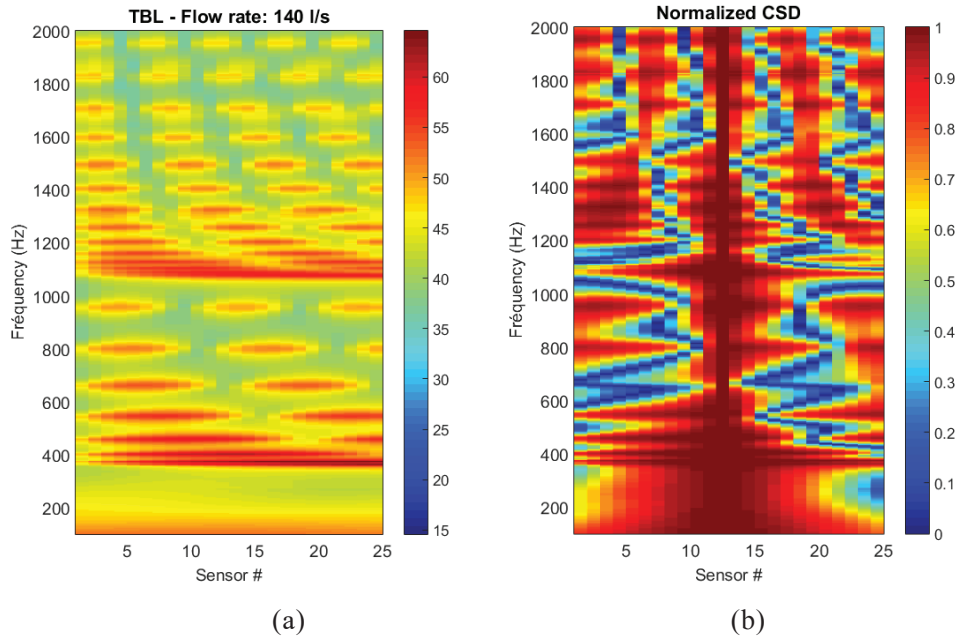


Figure 4. (a), Acceleration levels (ref. dB,  $1 \mu\text{m}\cdot\text{s}^{-2}\cdot\text{Hz}^{-0.5}$ ) measured by the sensor array when the pipe is excited by the turbulent flow. (b), Normalized cross spectrum density function of the shell displacement between sensor #12 and the sensor  $\#i \in [1,25]$ . Flow rate: 140 l/s.

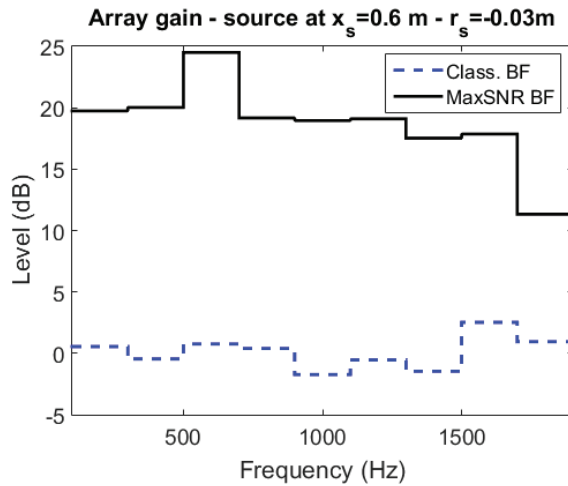


Figure 5. Array gain versus frequency.  
Wide band analysis of 500 Hz bandwidth

## 5. CONCLUSIONS

The present study was achieved in the framework of a novel non-intrusive vibro-acoustic technique for the detection of a sodium-water reaction in a sodium-cooled nuclear reactor steam generator. In order to study the efficiency of different beamforming treatments for increasing the SNR, a laboratory mock-up composed by a pipe coupled to a hydraulic circuit through two flanges has been developed. In parallel of the experimental investigations, the numerical simulation abilities are explored for assessing the performances of these treatments for different configurations. In the present paper, one has described the numerical vibro-acoustic tools that we have developed for predicting the vibratory response of the pipe excited by a monopole source or a turbulent boundary layer. These models allow us to realize virtual experiments mimicking the behavior of our laboratory test case. The virtual signals induced by the monopole source to be detected and by the turbulent flow are used to test the vibro-acoustic beamforming treatments. Different configurations of pipe, of array, of source and of flow can be easily considered with these virtual experiments. Obtained results show that the interest of the classical beamforming is weak for this configuration, whereas a significant gain is obtained with the



MaxSNR beamforming.

## ACKNOWLEDGEMENTS

This work was carried out in the framework of the LabEx CeLyA ("Centre Lyonnais d'Acoustique", ANR-10-LABX-60) and the Sodium Technology project of GEN4 program (R4G/TECNA) of the Nuclear Energy Division of CEA (CEA/DEN).

## REFERENCES

- [1] Moriot, J., Maxit L., Guyader, J.L., Gastaldi, O., Périsset, P., Use of beamforming for detecting an acoustic source inside a cylindrical shell filled with a heavy fluid, *Mech. Syst. Signal Process.*, vol. 52–53, pp. 645–662, Feb. 2015.
- [2] Moriot, J., Détection vibro-acoustique passive d'une réaction sodium-eau par formation de voies dans un générateur de vapeur d'un réacteur nucléaire à neutrons rapides refroidi au sodium, Thèse de doctorat, INSA de Lyon, 2013.
- [3] Manolakis, D.G., Ingle, V. K., Kogon, S., *Statistical and adaptive signal processing*. Boston, London: ARTECH House, 2005.
- [4] Maxit L., Ginoux J.M., Prediction of the vibro-acoustic behavior of a submerged shell non periodically stiffened by internal frames, *JASA*, 128 (2010) 137-151.
- [5] Tran-Van-Nhieu, M., Scattering from a ribbed finite cylindrical shell. *The Journal of the Acoustical Society of America*, 10 (2001), 2858–2866.
- [6] Goody, M.C., Empirical spectral model of surface pressure fluctuations, *AIAA J.*, 42 (2004) 1788–1794.
- [7] Chase, D.M., The character of the turbulent wall pressure spectrum at subconvective wavenumbers and a suggested comprehensive model, *J. Sound Vib.* 112 (1987) 125-147.
- [8] Maxit, L., Denis, V., Prediction of flow induced sound and vibration of periodically stiffened plate, *JASA*, 133 (2013) 146-160.
- [9] Meyer, V., Maxit, L., Renou, Y., Audoly, C., Vibroacoustic modelling of submerged stiffened cylindrical shells with internal structures under random excitations. *Proceedings of INTERNOISE 2016*, Hamburg, Germany, August 2016. 12 p.
- [10] Maxit, L., Meyer, V., Vibroacoustic modelling of periodically stiffened submerged cylindrical shells beneath a turbulent boundary layer, *Proceedings of INTERNOISE 2017*, Honk Kong, August 2017. 11 p.
- [11] Meyer, V., Development of a substructuring approach to model the vibroacoustic behavior of submerged stiffened cylindrical shells coupled to non-axisymmetric internal frames, PhD thesis, INSA Lyon, 2016.
- [12] Kassab, S., Vibroacoustic beamforming for the detection of an acoustic monopole inside a thin cylindrical shell coupled to a heavy fluid: Numerical and experimental developments, PhD thesis, Université de Lyon, INSA Lyon, Villeurbanne, France, 2018, 182 p. (in French).